0.5 for Z between 23 and 48. The ratio of $K\beta_3$ to $K\alpha_2$ rises fairly linearly with Z from 0.2 at $Z = 20$ to 0.4 at $Z = 80$ and that of $K\beta_1$ to $K\alpha_2$ is near zero at $Z = 29$ and rises linearly with Z to about 0.1 at $Z = 80$. Relative intensities of lines in the L spectrum are given by Goldberg (1961).

Green & Cosslett (1968) have made extensive measurements of the efficiency of the production of characteristic radiation for a number of targets and for a range of electron accelerating voltages. Their results can be expressed empirically in the form

$$N_K/4\pi = N_0/4\pi(E_0 - E_K - 1)^{1.63}, \qquad (4.2.1.1)$$

where $N_K/4\pi$ is the *generated* number of $K\alpha$ photons per steradian per incident electron, N_0 is a function of the atomic number of the target, E_0 is the electron energy in keV and E_K is the excitation potential in keV. It should be noted that $N_K/4\pi$ decreases with increasing Z.

For a copper target, this expression becomes

$$N_K/4\pi = 1.8 \times 10^{-6}\,(E_0 - 8.9)^{1.63} \qquad (4.2.1.2)$$

or

$$N'_K/4\pi = 1.1 \times 10^{10}\,(E_0 - 8.9)^{1.63}, \qquad (4.2.1.3)$$

where $N'_K/4\pi$ is the number of $K\alpha$ photons per steradian per second per milliampere of tube current.

These expressions are probably accurate to within a factor of 2 up to values of E_0/E_K of about 10. Guo & Wu (1985) found a linear relationship for the *emerging* number of photons with electron energy in the range $2 < E_0/E_K < 5$.

To obtain the number of photons that *emerge* from the target, the above expressions have to be corrected for absorption of the generated radiation in the target. The number of photons emerging at an angle φ to the surface, for normal electron incidence, is usually written

$$N_\varphi/4\pi = f(\chi)N/4\pi, \qquad (4.2.1.4)$$

where $\chi = (\mu/\rho)\,\mathrm{cosec}\,\varphi$ (Castaing & Descamps, 1955). Green (1963) gives experimental values of the correction factor $f(\chi)$ for a series of targets over a range of electron energies. His curves for a copper target are given in Fig. 4.2.1.1. It will be noticed that the correction factor increases with increasing electron energy since the effective depth of X-ray generation increases with voltage. As a result, curves of N_φ as a function of E_0 have a broad maximum that is displaced towards lower voltages as φ decreases, as shown in the experimental curves for copper K radiation due to Metchnik & Tomlin (1963) (Fig. 4.2.1.2). For very small take-off angles, therefore, X-ray tubes should be operated at lower than customary voltages. Note that the values in Fig. 4.2.1.2 agree to within $\sim 40\%$ with those of Green & Cosslett. $f(\chi)$ at constant E_0/E_K increases with increasing Z, thus partly compensating for the decrease in N_K, especially at small values of φ. A recent re-examination of the characteristic X-ray flux from Cr, Cu, Mo, Ag and W targets has been carried out by Honkimaki, Sleight & Suortti (1990).

4.2.1.2. *The continuous spectrum*

The shape of the continuous spectrum from a thick target is very simple: I_ν, the energy per unit frequency band in the spectrum, is given by the expression derived by Kramers (1923):

$$I_\nu = AZ(\nu_0 - \nu) + BZ^2, \qquad (4.2.1.5)$$

where Z is the atomic number of the target and A and B are constants independent of the applied voltage E_0. B/A is of the order of 0.0025 so that the term in Z^2 can usually be neglected (Fig. 4.2.1.3). ν_0 is the maximum frequency in the spectrum, *i.e.* the Duane–Hunt limit at which the entire energy of the bombarding electrons is converted into the quantum energy of the emitted photon, where

$$H\nu_0 = hc/\lambda_0 = E_0. \qquad (4.2.1.6)$$

Using the latest adjusted values of the fundamental constants (Cohen & Taylor, 1987):

$$hc = 1.23984244 \pm 0.00000037 \times 10^{-6}\ \text{eV m}$$
$$= 12.3984244 \pm 0.0000037\ \text{keV Å}.$$

Equation (4.2.1.5) can be rewritten in a number of forms. If $\mathrm{d}N_E$ is the number of photons of energy E per incident electron,

$$\mathrm{d}N_E = bZ(E_0/E - 1)\ \mathrm{d}E, \qquad (4.2.1.7)$$

where $b \sim 2 \times 10^{-9}$ photons eV^{-1} $\mathrm{electron}^{-1}$, and is known as Kramer's constant.

From (4.2.1.7), it follows that the total energy in the continuous spectrum per electron is

$$\int_0^{E_0} E\ \mathrm{d}N_E = bZE_0^2/2. \qquad (4.2.1.8)$$

Since the energy of the bombarding electron is E_0, the efficiency of production of the continuous radiation is

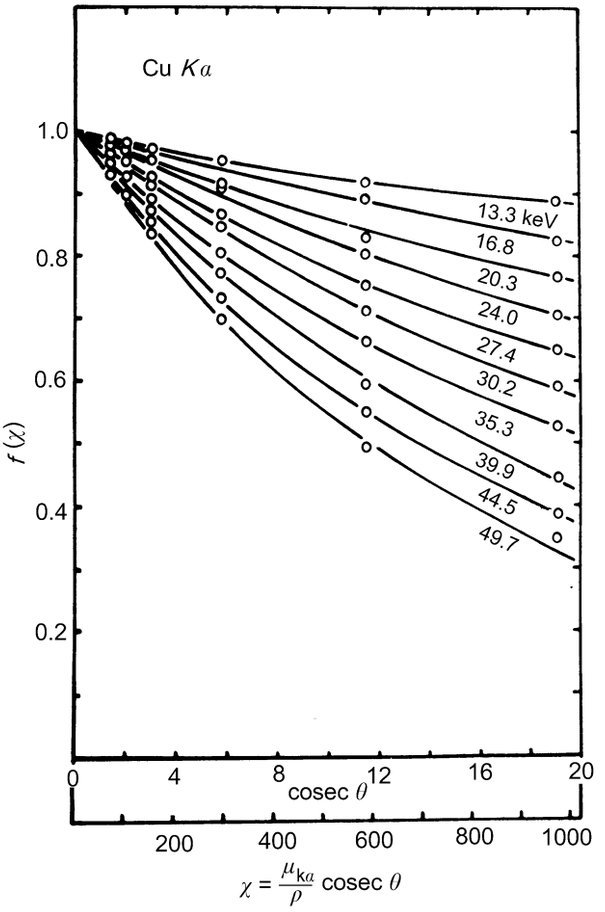

Fig. 4.2.1.1. $f(\chi)$ curves for Cu K-L_3 at a series of different accelerating voltages (in kV). From Green (1963).

$$\eta_c = bZE_0/2. \quad (4.2.1.9)$$

Crystallographers are more accustomed to thinking of the spectrum in terms of wavelength. Equation (4.2.1.7) can be transformed into

$$dN_\lambda = hcbZ(1/\lambda^2 - 1/\lambda\lambda_0)\, d\lambda, \quad (4.2.1.10)$$

which has a maximum at $\lambda = 2\lambda_0$. In practice, the *emerging* spectrum is modified by target absorption, which is greatest for the longer wavelengths and moves the maximum more nearly to $1.5\lambda_0$.

It is of interest to compare the X-ray flux in a narrow wavelength band selected by an appropriate monochromator with the flux in a characteristic spectral line, in order to examine the practicability of XAFS (X-ray absorption fine-structure spectroscopy) or optimized anomalous-dispersion diffractometry experiments. For these purposes, the maximum permissible wavelength band is about 10^{-3} Å. From equation (4.2.1.10), we see that, for a tungsten-target X-ray tube operated at 80 kV, dN_λ is about 1.1×10^{-5} photons with the $K\alpha$ energy electron^{-1} steradian^{-1} $(10^{-3}\,\delta\lambda/\lambda)^{-1}$ for an X-ray wavelength in the neighbourhood of 1.5 Å. By comparison, from equation (4.2.1.2), a copper-target tube operated at 40 kV produces about 5×10^{-4} $K\alpha$ photons electron^{-1} steradian^{-1}. In spite of this shortcoming by a factor of about 45, laboratory XAFS experiments are sufficiently common to have merited at least one specialized conference (Stern, 1980; see also Tohji, Udagawa, Kawasaki & Masuda, 1983; Sakurai, 1993; Sakurai & Sakurai, 1994).

The use of continuous radiation for diffraction experiments is complicated by the fact that the radiation is polarized. The degree of polarization may be defined as

$$p = (I_\parallel - I_\perp)/(I_\parallel + I_\perp), \quad (4.2.1.11)$$

where $I_\parallel$ and $I_\perp$ are the intensities of radiation with the electric vector parallel and perpendicular to the plane containing the incident electrons and the direction of the emitted photons. For an angle of $\pi/2$ between the electrons and the emitted beam, p varies smoothly through the spectrum; it is negative for the softest radiation, approximately zero at $\nu/\nu_0 \sim 0.1$ and reaches values between +0.7 and +0.9 near the Duane–Hunt limit (Kirkpatrick & Wiedmann, 1945). Since practical use of white radiation is likely to be in the vicinity of $\nu/\nu_0 \sim 0.1$, the effect is not a large one.

It should also be noted that the spatial distribution of the white spectrum, even after correction for absorption in the target, is not isotropic. The intensity has a maximum at about 50° to the electron beam and non-zero minima at 0 and 180° to that beam (Stephenson, 1957).

4.2.1.3. *X-ray tubes*

The commonest source of X-rays is the high-vacuum, or Coolidge, X-ray tube, which may be either demountable and pumped continuously when in operation or permanently sealed after evacuation. The vacuum tube contains an electron gun that incorporates a thermionic cathode, which produces a well defined electron beam that is accelerated towards the anode or target, formerly often called the anticathode. In most X-ray tubes intended for crystallographic purposes, the anode is massive, *i.e.* its thickness is large compared with the range of the electrons; it is usually water-cooled and its surface is normal to the incident electron beam. Usually, it is desirable for the X-ray source to be small (between 25 μm and 1 mm square) and for the X-ray intensity from the tube to be the maximum possible for the amount of power that can be dissipated in the target. These objectives are best achieved by

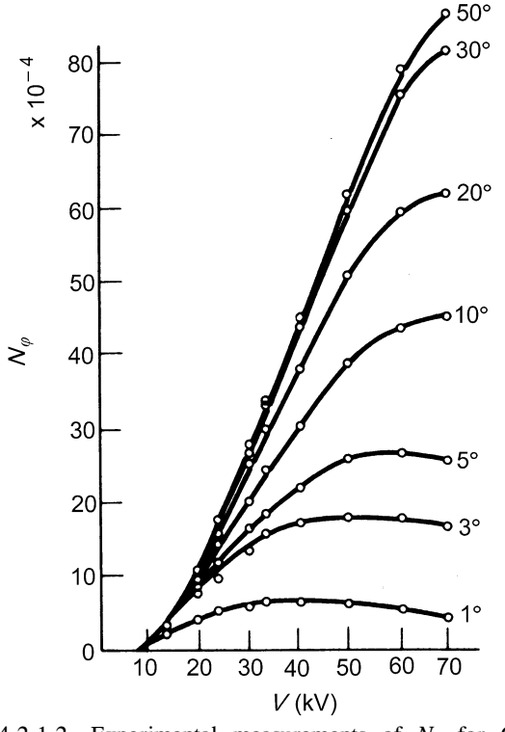

Fig. 4.2.1.2. Experimental measurements of N_φ for Cu K-L_3 as functions of the accelerating voltage for different take-off angles. From Metchnik & Tomlin (1963).

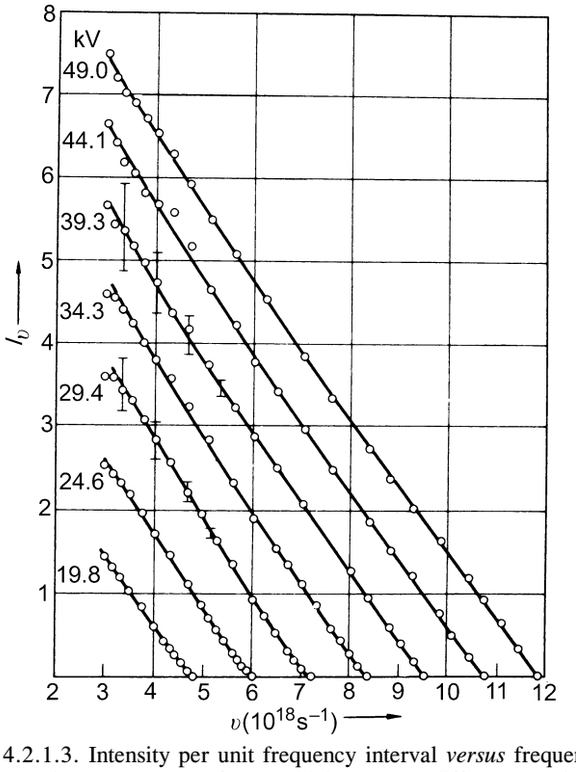

Fig. 4.2.1.3. Intensity per unit frequency interval *versus* frequency in the continuous spectrum from a thick target at different accelerating voltages. From Kuhlenkampff & Schmidt (1943).

references